JOURNAL OF Materials CHEMISTRY

Synthesis and excited-state photodynamics of perylene–porphyrin dyads Part 3.† Effects of perylene, linker, and connectivity on ultrafast energy transfer

Sung Ik Yang,[a] Robin K. Lammi,[a] Sreedharan Prathapan,[b]‡ Mark A. Miller,[b] Jyoti Seth,[c] James R. Diers,[c] David F. Bocian,*[c] Jonathan S. Lindsey*[b] and Dewey Holten*[a]

[a]*Department of Chemistry, Washington University, St. Louis, Missouri, 63130-4899*
[b]*Department of Chemistry, North Carolina State University, Raleigh, North Carolina, 27695-8204*
[c]*Department of Chemistry, University of California, Riverside, California, 92521-0403*

Received 1st March 2001, Accepted 15th June 2001
First published as an Advance Article on the web 3rd August 2001

New perylene–porphyrin dyads have been designed that exhibit superior light-harvesting and energy-utilization activity compared with earlier generations of structurally related dyads. The new dyads consist of a perylene mono(imide) dye (PMI) connected to a porphyrin (Por) *via* an ethynylphenyl (ep) linker. The PMI–ep–Por arrays were prepared with the porphyrin as either a zinc or magnesium complex (Por = Zn or Mg) or a free-base form (Por = Fb). The absorption properties of the perylene complement those of the porphyrin. Following excitation of the perylene (forming PMI*) in toluene, each array exhibits ultrafast ($k_{ENT} \geqslant (0.5\ ps)^{-1}$) and essentially quantitative energy transfer from PMI* to the ground-state porphyrin (forming Por*). In each of the arrays, the properties of the excited porphyrin (lifetime, fluorescence yield, *etc.*) are basically unperturbed from those of the isolated pigment. Thus, following energy transfer, the excited porphyrin is not quenched by deleterious reactions involving the perylene accessory unit that would otherwise limit the ability of Por* to emit light or transfer energy to another stage in a molecular photonic device. Collectively, the PMI–ep–Por dyads represent the successful result of a molecular design strategy to produce arrays with excellent properties for use as light-input and energy-transduction elements for applications in molecular optoelectronics.

Introduction

Tetrapyrrole–protein complexes carry out a variety of biological functions that involve molecular transport, catalysis, light harvesting, energy migration, and charge transfer. This diverse behavior arises in part from the tunability of the electronic properties of tetrapyrroles through variations in central metal, peripheral groups, axial ligands, and π-system conjugation. Such flexibility has prompted the incorporation of porphyrinic chromophores in biomimetic energy-harvesting/transduction systems and in prototypical molecular-optoelectronics architectures. The properties of these constructs can be further enhanced *via* the use of accessory pigments in conjunction with porphyrins. This combination permits more efficient use of the solar spectrum for light harvesting, increases selectivity in the excitation of one component over another, and expands the available redox span for charge-transfer processes.

The ability to discriminate between energy transfer and charge (hole/electron) transfer is an important consideration in the design of units consisting of porphyrins and accessory pigments. Energy transfer is essential for light harvesting, whereas charge transfer is more important for light-induced switching. In the latter area, Wasielewski and coworkers have pioneered the use of perylenes as electron acceptors from photoexcited porphyrins and as sensors for nearby charge-separated states.[1–3] Although perylene dyes have been used extensively as light absorbers, energy-transfer agents, and charge carriers,[4–12] there are only a limited number of examples in which a perylene has been employed to deliver absorbed light energy to a covalently attached porphyrin.[2,13–15] Several of these arrays belong to a class of dyads that we recently prepared and characterized; these dyads consist of a perylene diimide dye (PDI), a diphenylethyne linker (pep), and either a zinc, magnesium, or free-base porphyrin (Por = Zn, Mg, Fb).[14,15] These PDI–pep–Por dyads are shown in Chart 1.

Our studies of the PDI–pep–Por arrays revealed a diversity of photoinduced energy-transfer and charge-transfer phenomena. Some of these processes are illustrated in the generalized state/kinetic diagram in Fig. 1A. For example, for PDI–pep–Fb in toluene, energy transfer from the photoexcited perylene (PDI*) to the porphyrin (forming Fb*) is rapid (~3 ps) and efficient (85%). This overall process is made effectively quantitative because hole transfer involving the remaining 15% of PDI* to form PDI^-–pep–Fb^+ primarily gives Fb* by charge recombination. The resultant Fb* state has properties very similar to those of the isolated porphyrin. In contrast, for PDI–pep–Mg, the charge-separated state PDI^-–pep–Mg^+ is produced in 50% yield in ~2.5 ps upon excitation of the perylene and quantitatively in ~150 ps upon excitation of the porphyrin, and then decays in >10 ns in toluene and <0.5 ns in acetonitrile. The different behavior of these dyads arises largely because the redox properties of the respective porphyrins afford different energies of the PDI^-–pep–Por^+ charge-separated states with respect to the other electronic states in each dyad.[14,15]

We wished to further manipulate the rates and yields of the energy-transfer and charge-transfer processes in perylene–porphyrin dyads. A number of design considerations led us to synthesize the PMI–ep–Por (Por = Zn, Mg, Fb) class of dyads shown in Chart 1. These arrays have three fundamental

†For Parts 1 and 2, see refs. 14 and 15 respectively.
‡*Permanent address*: Department of Applied Chemistry, Cochin University of Science and Technology, Cochin, India 682022.

 DOI: 10.1039/b102741g

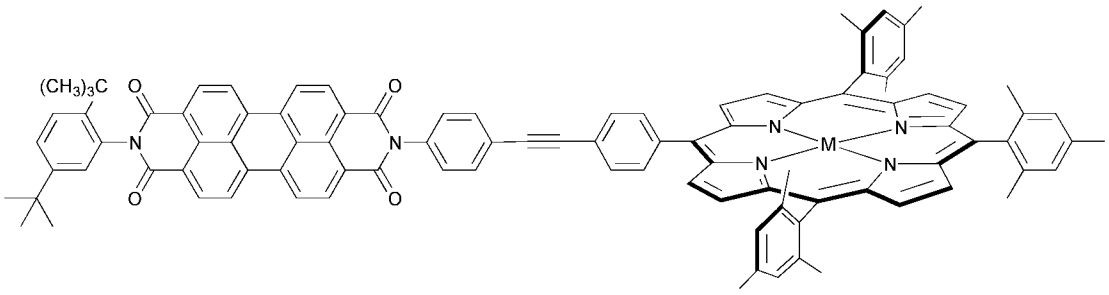

PDI-pep-Zn (M = Zn^{2+}) PDI-pep-Mg (M = Mg^{2+}) PDI-pep-Fb (M = $2H^{+}$)

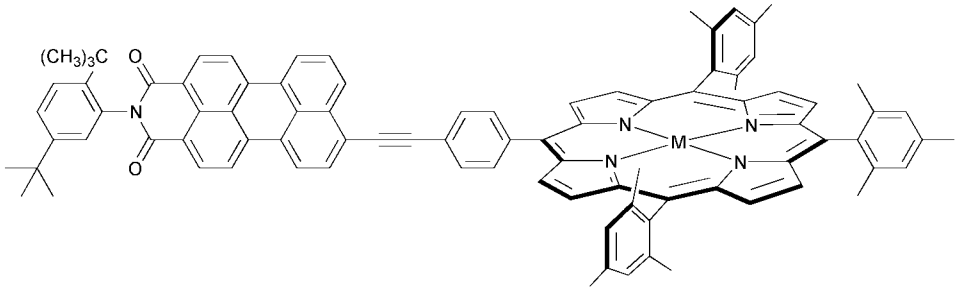

PMI-ep-Zn (M = Zn^{2+}) PMI-ep-Mg (M = Mg^{2+}) PMI-ep-Fb (M = $2H^{+}$)

Chart 1

structural changes compared with their PDI–pep–Por analogs: (1) the perylene diimide is replaced with a monoimide (PMI), (2) the linker is shortened from diphenylethyne to phenylethyne (ep), and (3) the site of attachment of the linker to the perylene imide unit is shifted from an imide nitrogen to the C9 position of the perylene core. The rationale for making these structural changes is described below.

The type of perylene was altered to make this moiety more difficult to reduce. This characteristic should increase the energies of the PMI^{-}–ep–Por^{+} charge-separated states with respect to the analogous states in the PDI–pep–Por dyads, thereby altering the thermodynamics and rates of the charge-transfer reactions (which also depend on the solvent polarity). This point is illustrated in Fig. 1B for the PMI–ep–Por dyads in nonpolar media.

The linker was shortened to increase the rates of the energy-transfer and charge-transfer processes.

The rationale for changing the linker attachment site follows from our studies on excited-state energy transfer[16–21] and ground-state hole/electron hopping[22] between porphyrins joined *via* diarylethyne linkers. Photoinduced energy transfer occurs primarily by a through-bond (rather than through-space) mechanism, and significant changes in rate can be achieved by altering the attachment site of the linker to the porphyrin (and *vice versa*).[16,17,19,21] The effects of attachment site on inter-porphyrin electronic communication correlate with the electron densities in the frontier molecular orbitals of the porphyrin and linker. These same principles should apply for accessory chromophores. Indeed, one of the many favorable characteristics of perylene imide dyes[14] is the uneven distribution of electron density on different atoms as shown by calculations and photophysical studies. In particular, the orbital coefficients are much higher at the perylene 3, 4, 9, and 10 positions than at the *N*-imide positions.[23,24] Thus, we expected that changing the site of linker attachment from the imide nitrogen in the PDI–pep–Por dyads to the perylene 9-position in the PMI–ep–Por arrays should significantly increase electronic communication with the porphyrin, especially in combination with the shorter linker (Chart 1).

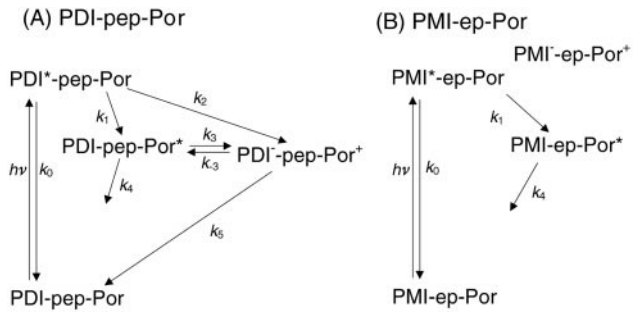

Fig. 1 Generalized state/kinetic diagrams for the two families of perylene–porphyrin dyads.

The results reported herein indicate that our design objectives for the PMI–ep–Por (Por = Zn, Mg, Fb) dyads have been successfully achieved. In particular, this paper describes studies on the PMI–ep–Por arrays in toluene, where the dominant process is found to be subpicosecond energy transfer from perylene to porphyrin (ideal for light-harvesting applications). A future paper will describe results for these dyads in acetonitrile, where ultrafast charge transfer and charge recombination dominate (applicable for light-induced switching functions). Collectively, the PDI–pep–Por and PMI–ep–Por arrays represent a family of related bichromophoric units with robust properties that can be utilized for a variety of applications in molecular photonics.

Results

Synthesis

The synthesis of the dyads PMI–ep–Zn and PMI–ep–Fb has been previously described.[13] Treatment of PMI–ep–Fb with the heterogeneous magnesium insertion conditions (MgI_2 and *N,N*-diisopropylethylamine in CH_2Cl_2 at room temperature)[25] afforded the desired PMI–ep–Mg in 88% yield. The reference compounds PMI-m,[26] PMI-e,[13] and PMI-ep,[13] ZnU′,[27] MgU′,[18] FbU′[28] have been synthesized previously (Chart 2).

Redox properties

Electrochemical data for the PMI–ep–Por (Por = Zn, Mg, Fb) dyads and the PMI-m and PMI-e reference compounds are summarized in Table 1. For comparison, this table also

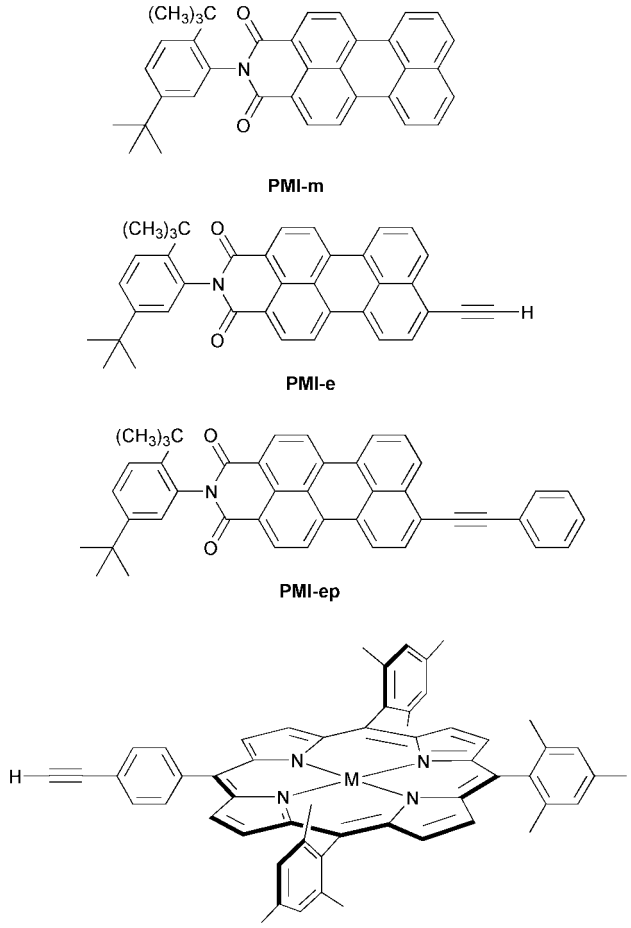

Chart 2

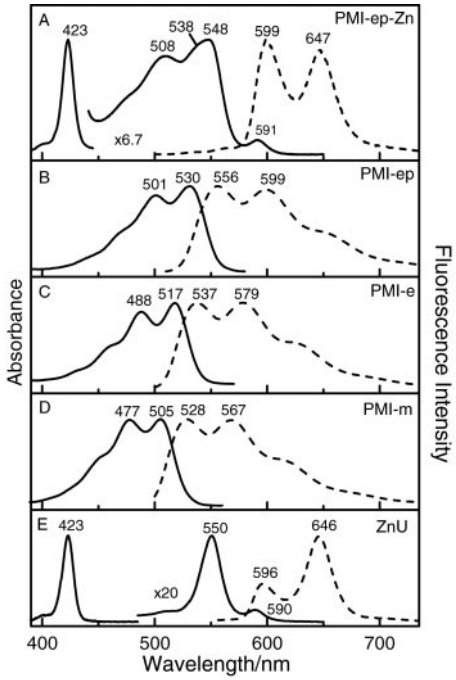

Fig. 2 Absorption spectra and fluorescence spectra for PMI–ep–Zn and reference compounds in toluene at room temperature. The emission was elicited by perylene excitation at 490 nm. An identical emission spectrum for the dyad was obtained using porphyrin Soret (420 nm) excitation.

includes data for the related perylene diimide-containing dyads PDI–pep–Por and the PDI-m reference compound described previously.[14,15] Half-wave potentials ($E_{½}$) were determined by square-wave voltammetry (frequency 10 Hz). The isolated perylene dyes exhibit one oxidation wave and two reduction waves in the +1.5 to −2.0 V range. The $E_{½}$ values of the perylene units in the PMI–ep–Por dyads are generally similar to those of the perylene monoimide unit PMI.[29] Porphyrin units in the dyads exhibit two oxidation and two reduction waves in the +1.5 to −2.0 V range and have $E_{½}$ values similar to those observed for other tetraarylporphyrins.[30] In general, these data are indicative of relatively weak ground-state interactions between the perylene and porphyrin constituents of the dyads.

The most noteworthy characteristic of the redox properties of the perylene dyes is the substantial difference in both the oxidation and reduction potentials of the monoimide (PMI-m, PMI-e, PMI–ep–Por) *versus* diimide (PDI-m, PDI–pep–Por) forms. The oxidation potentials of the monoimides are 250–350 mV less positive than those of the diimides.[31] The differences in the reduction potentials for the two types of complexes are even larger, with those of the monoimide lying 350–450 mV more negative than those of the diimides.

Absorption spectra

Ground-state electronic absorption spectra for PMI–ep–Zn and several reference compounds are shown in Fig. 2. Spectra for all three PMI–ep–Por (Por = Zn, Mg, Fb) dyads are shown in Fig. 3. For comparison, the latter figure also shows spectra for the corresponding PDI–pep–Por dyads. A key finding is that the spectral characteristics of the PMI–ep–Por dyads deviate substantially from the sum of the spectra of isolated reference compounds. This represents a major distinction from the PDI–pep–Por dyads, for which the spectral properties of the PDI and Por units in the arrays are essentially identical to those of the isolated chromophores.[14,15] These absorption characteristics (and related fluorescence properties) are indicative of much stronger (excited-state) perylene–porphyrin electronic communication in the PMI–ep–Por *versus* PDI–pep–Por arrays. These findings are described in more detail below.

Table 1 Half-wave potentials ($E_{½}$) for the perylene-containing compounds[a]

	Oxidation potentials/V			Reduction potentials/V			
	Perylene	ZnPor		Perylene		ZnPor	
		$E_{½}$ (1)	$E_{½}$ (2)	$E_{½}$ (1)	$E_{½}$ (2)	$E_{½}$ (1)	$E_{½}$ (2)
PMI-m	+1.05	—	—	−1.24[b]	−1.79[b]	—	—
PMI-e	+1.10	—	—	−1.16	−1.65	—	—
PMI–ep–Zn	+1.10	+0.50	+0.88	−1.14	−1.60	−1.75	−2.18
PDI-m[c]	+1.36			−0.81	−1.07		
PDI–pep–Zn[c]	+1.40	+0.52	+0.90	−0.77	−1.06	−1.71	−2.12

[a]Obtained in butyronitrile containing 0.1 M TBAH. $E_{½}$ *vs* Ag/Ag^{+}; $E_{½}$ of $FeCp_2/FeCp_2^{+}$ = 0.19 V. The $E_{½}$ values are obtained from square wave voltammetry (frequency = 10 Hz). Values are ± 0.01 V. [b]For comparison, see ref. 29. [c]From ref. 14.

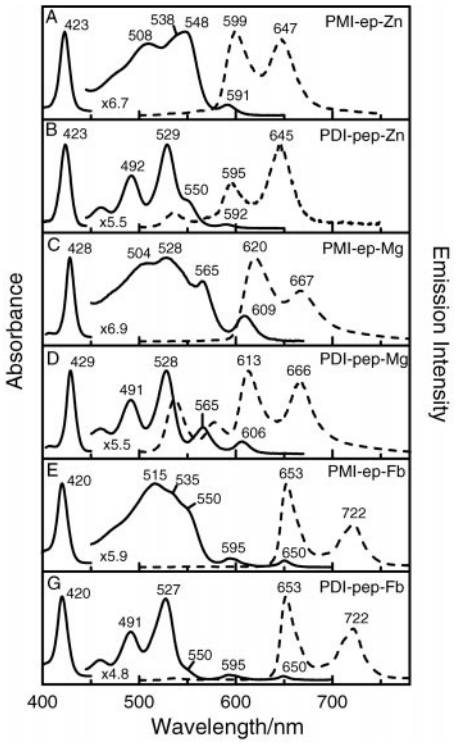

Fig. 3 Absorption and fluorescence spectra for PMI–ep–Por and PDI–pep–Por arrays (Por = Zn, Mg, Fb). Conditions as in Fig. 2.

The perylene imide unit in the PMI–ep–Por dyads and in the reference compounds exhibits a progression of (at least) three resolved absorption bands designated (2,0), (1,0) and (0,0). These features lie at ~450, 477, and 505 nm, respectively, for the benchmark PMI-m monomer (Fig. 2D). Each of these bands red shifts ~10 nm with successive addition of the ethyne group to make PMI-e, the phenyl group to make PMI-ep, and finally the Zn porphyrin to complete the construction of the PMI–ep–Zn dyad (Fig. 2). Similar effects are found for PMI–ep–Mg and PMI–ep–Fb. However, the perylene absorption features do not appear to be at precisely the same positions in the three PMI–ep–Por dyads, even after considering the effects of overlap with one or more of the porphyrin Q bands described below (Fig. 3A, C, E).[32]

The absorption spectra of the porphyrin components of the arrays and the reference monomers contain the typical features, namely a strong, near-UV Soret (B) band (420–430 nm) and a series of weaker, visible Q bands (500–650 nm). The B(0,0), Q(2,0), Q(1,0) and Q(0,0) bands lie at approximately 423, 510, 550, and 590 nm, respectively, for the ZnU′ reference porphyrin (Fig. 2E). These features have approximately the same positions in the PMI–ep–Zn dyad (Fig. 2A). However, the Q-band intensity ratio may be slightly different in this dyad relative to PDI–pep–Zn (Fig. 3A *versus* Fig. 3B), which has identical porphyrin features to those of ZnU′ (Fig. 2E).[33]

Analogous characteristics are seen for PMI–ep–Mg, for which the 565 nm position of the Q(1,0) band overlaps less with the perylene origin transition (Fig. 3C). In addition, the porphyrin Q(0,0) band at 609 nm for PMI–ep–Mg is red-shifted ~3 nm from the position in PDI–pep–Mg (Fig. 3C *versus* Fig. 3D), which is identical to that in the MgU′ monomer.[14] In contrast, the Fb porphyrin $Q_x(0,0)$ and $Q_x(1,0)$ bands (650 and 595 nm) have the same positions and intensity ratio in PMI–ep–Fb, PDI–pep–Fb, and FbU′ (Fig. 3E, 3F and ref. 20). The same is likely also true of the Fb porphyrin $Q_y(0,0)$ and $Q_y(1,0)$ bands in the dyad (expected at ~550 and ~515 nm); however, these features partially overlap the perylene features so an exact comparison cannot be made.

The picture that emerges from the absorption features of the PMI–ep–Por dyads is as follows. (1) The absorption properties of the porphyrin component in the PMI–ep–Por dyads are not altered as substantially as those of the PMI components relative to the respective reference monomers. (2) The perturbation of the absorption characteristics of the PMI components is predominantly due to excited-state effects. This latter point follows from the finding of approximately the same difference in ground-state reduction potentials in the PMI–ep–Zn *versus* PDI–pep–Zn dyads as in the PMI-m *versus* PDI-m monomers; accordingly, the ground-state coupling effects in the PMI–ep–Por (or PDI–pep–Por) dyads are not particularly pronounced. Thus, the perturbations on the absorption spectra (which reflect differences between the ground and excited states) must reflect largely excited-state effects. (3) The perturbations on the excited-state properties of the PMI components depend in detail on the nature of the porphyrin. This latter property is even more apparent in the fluorescence data described below.

Fluorescence spectra, quantum yields, and lifetimes

Emission spectra of the various compounds in toluene are shown in Fig. 2 and 3 (dashed spectra). There are two overriding aspects of the fluorescence properties of the three PMI–ep–Por arrays in toluene: (1) the emission of the dyads occurs almost exclusively from the porphyrin, even if the perylene is preferentially excited. This observation is indicative of efficient PMI*–ep–Por → PMI–ep–Por* energy transfer. (2) The porphyrin fluorescence properties (spectral intensity ratios, quantum yields, lifetimes) for the dyads are all perturbed to a degree from those of the isolated chromophores, and the perturbations are larger for the metalloporphyrin-containing dyads than for PMI–ep–Fb. These altered emission characteristics likely arise from the same strong porphyrin–perylene electronic interactions indicated by the absorption spectra. These findings, which reflect both similarities and differences with the PDI–pep–Por dyads characterized previously,[14,15] are described in more detail in the sections below.

PMI–ep–Zn. Fig. 2 shows the fluorescence spectra of PMI–ep–Zn and several reference compounds in toluene (dashed spectra). In analogy with the absorption spectra, the perylene (0,0), (0,1) and (0,2) emission bands at 528, 567, and ~620 nm for PMI-m progressively red-shift upon addition of the ethyne group to make PMI-e and then the phenyl ring to make PMI-ep (Fig. 2B–D). These spectral effects are accompanied by a change in the PMI* radiative rate constant, as is deduced from the emission yields and lifetimes (Table 2). In particular, along the series PMI-m, PMI-e, PMI-ep, the perylene radiative rate constant $k_f = \Phi_f/\tau$ progressively changes from 0.99/4.8 ns ≈ $(4.8\ \text{ns})^{-1}$ to 0.97/3.9 ns ≈ $(4.0\ \text{ns})^{-1}$ to 0.95/3.4 ns ≈ $(3.6\ \text{ns})^{-1}$.

Upon addition of the porphyrin to make PMI–ep–Zn, the perylene emission is almost completely quenched,[34] but the porphyrin Q(0,0) and Q(0,1) fluorescence features at ~600 and ~650 nm are readily apparent (Fig. 2A). Comparison of optically matched samples at 490 nm (where PMI absorbs >100 times more than the porphyrin) reveals that the perylene fluorescence yield for PMI–ep–Zn is reduced to $\Phi_f < 0.001$ from 0.99 for PMI-m (Table 2). In contrast, the Zn* fluorescence intensity obtained using perylene excitation ($\Phi_f = 0.072$) is comparable to that found using direct excitation of the porphyrin in the Soret band at 420 nm (0.068) or the Q(1,0) band at 550 nm (0.070) (Table 2). Collectively, these data demonstrate that energy transfer from PMI* to the ground-state porphyrin to form Zn* is essentially quantitative.

Interestingly, comparison of optically matched samples at 420 nm shows that the Zn* fluorescence yield in the dyad is *increased* about two-fold from that in the ZnU′ reference monomer (Table 2). The ratio of the porphyrin Q(0,0) and

Table 2 Photophysical properties of PMI–ep–Por dyads and reference compounds[a]

	Perylene excited-state decay		Porphyrin excited-state decay	
Compound	τ/ps	Φ_f	τ/ns	Φ_f
Dyads				
PMI–ep–Zn	$\leqslant 0.4$	<0.001	2.3 ± 0.2^b	0.070 ± 0.002^c
PMI–ep–Mg	$\leqslant 0.4$	<0.001	9.1 ± 0.9^d	0.24 ± 0.01
PMI–ep–Fb	$\leqslant 0.4$	<0.001	12.3 ± 0.9^e	0.14 ± 0.01
Monomers				
PMI-m	4800 ± 100^f	0.99 ± 0.01^f		
PMI-e	3900 ± 100	0.97 ± 0.01		
PMI-ep	3400 ± 100	0.95 ± 0.01		
FbU′			13.3 ± 0.9^g	0.12 ± 0.01^g
ZnU′			2.4 ± 0.2^h	0.035 ± 0.00^h
MgU′			10.0 ± 0.8^i	0.16 ± 0.01^i

[a]All measurements in toluene at room temperature. [b]Average value from fluorescence (2.4 ns) and transient absorption (2.1 and 2.3 ns). [c]Average value from 420 nm porphyrin excitation (0.068), 550 nm porphyrin excitation (0.070), and 490 nm perylene excitation (0.072). [d]The fluorescence lifetime is 1.9 ns in iodobenzene. [e]The fluorescence lifetime is 1.4 ns in iodobenzene. [f]In iodobenzene, $\tau = 1.3$ ns (measured by transient absorption) and $\Phi_f = 0.46$. [g]From ref. 33*b*. [h]From refs. 16, 33*b*. [i]From ref. 18.

Q(0,1) emission features is also altered in a related manner in the dyad *versus* the monomer (Fig. 2A *versus* Fig. 2E). These two sets of data are self-consistent in reflecting an approximately two-fold increase in the porphyrin radiative rate constant k_f in PMI–ep–Zn *versus* ZnU′.[35]

PMI–ep–Mg. Analogous fluorescence properties are exhibited by PMI–ep–Mg in toluene. Quantitative PMI*–ep–Mg → PMI–ep–Mg* energy transfer is indicated by (1) the >1000-fold reduction in PMI* fluorescence yield in the dyad relative to PMI-m, and (2) the fluorescence yields obtained using perylene (490 nm) or porphyrin (420 nm) excitation (Table 2). Strong perylene–porphyrin interactions in PMI–ep–Mg (but perhaps not as strong as in PMI–ep–Zn) are indicated by an increase in radiative rate constant k_f of ~1.5-fold compared to MgU′, as assessed from both the emission yield/lifetime results and the Q(0,0)/Q(0,1) ratio in the fluorescence spectra.[36]

PMI–ep–Fb. Similar fluorescence properties are found for PMI–ep–Fb in toluene. As is the case for the other two dyads, quantitative PMI*–ep–Fb → PMI–ep–Fb* energy transfer is indicated by the combination of (1) the >1000-fold reduced PMI* emission yield relative to that in PMI-e (Table 2), (2) the exclusive presence of Fb* emission using perylene excitation (namely the Q(0,0) and Q(0,1) features at 653 and 722 nm (Fig. 3E)), and (3) the same porphyrin emission yield ($\Phi_f = 0.14$) with excitation of perylene (490 nm) and porphyrin (420 nm) (Table 2). It is also noteworthy that the fluorescence yield/lifetime date and the band-intensity ratios in the optical spectra are only weakly perturbed (if at all) in the dyad *versus* FbU′. These data taken together with the analogous observations described above for the other compounds show that porphyrin–perylene electronic interactions are weaker in PMI–ep–Fb than in the metalloporphyrin-containing dyads.[37]

Time-resolved absorption spectra

PMI–ep–Zn. Fig. 4A shows transient absorption spectra for PMI–ep–Zn in toluene. Data were acquired using 130 fs flashes at 490 nm (predominantly exciting the perylene), or at 550 nm,

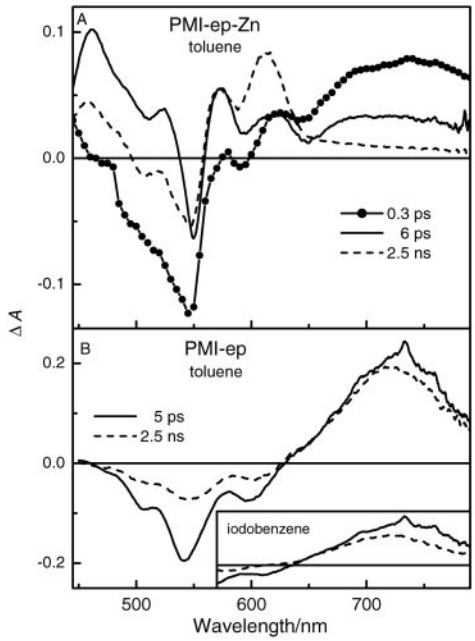

Fig. 4 Time-resolved absorbance difference spectra at room temperature for (a) PMI–ep–Zn and (b) PMI-ep at the specified time delays in the solvents indicated. Data from 450 to 670 nm were obtained using excitation with a 130 fs 490 nm flash, and data from 570 to 790 nm with a 550 nm flash; the spectra agreed well in the region of overlap (after correcting for differences in sample concentrations and extent of excitation).

with excellent agreement in regions of overlap (570–670 nm). The spectrum at 0.3 ps is due mainly to the perylene excited state PMI*, because it contains all the features expected based on the static absorption and fluorescence spectra in Fig. 2A and B. These characteristics are bleachings of the perylene (2,0), (1,0), and (0,0) ground-state absorption bands at ~475, ~510, and ~550 nm, along with the corresponding (0,0), (0,1), and (0,2) PMI* stimulated emission bands at ~550, ~615, and ~670 nm. The decay of PMI* is extremely fast ($\leqslant 0.4$ ps) and occurs essentially quantitatively by PMI*–ep–Zn → PMI–ep–Zn* energy transfer, based on static emission data and the time-resolved spectral data. Consequently, although the 0.3 ps spectrum is due predominantly to PMI*, it also contains small contributions from Zn* (best seen in the 6 ps spectrum) because energy transfer has occurred to some extent even at this early time.[38]

The spectrum of Zn* is shown at 6 ps (Fig. 4A, solid), and contains all the features expected based on the static absorption and emission spectra in Fig. 2A. These characteristics are bleaching of the Q(2,0) and Q(1,0) ground-state absorption bands at 515 and 550 nm, combined Q(0,0) bleaching and Zn* stimulated emission at 595 nm, and Q(0,1) stimulated emission at ~645 nm. The excited porphyrin decays with a time constant of ~2.3 ns, revealing the spectrum at 2.5 ns (Fig. 4A, dashed). Even after considering the residual Zn* contributions, it is clear that the direct or consequent product(s) of Zn* decay give mixed porphyrin–perylene characteristics to the long-time spectrum. These features include (1) bleachings in the perylene bands (as in the 0.3 ps PMI* spectrum) but without PMI* stimulated emission, (2) bleachings associated with the porphyrin component of the dyad (as in the 6 ps Zn* spectrum), and (3) an absorption band at ~615 nm that is not seen in the spectra at earlier times.

At first glance, the 2.5 ns spectrum appears to be consistent with the PMI^-–ep–Zn^+ charge-separated state. In particular, there are similarities to the spectrum of this state observed for this dyad in acetonitrile, which include a band at ~640 nm that is also seen in the PMI^- spectrum obtained

electrochemically.)[39] However, the fluorescence yield and lifetime data show that PMI^{-}–ep–Zn^{+} does not form to any appreciable extent from either PMI* or Zn*. Rather, PMI* decays essentially quantitatively to Zn* by energy transfer, and Zn* decays basically as it does in the isolated chromophore (80–90% by intersystem crossing to the Zn^{T} triplet excited state[40]). Thus, the 2.5 ns spectrum in the dyad could partially represent Zn^{T}, but with some PMI^{-}–ep–Zn^{+} charge-transfer character or other perturbations from the typical[41a] Zn^{T} spectrum (as a consequence of strong perylene–porphyrin electronic interactions). Another possibility is that Zn^{T} undergoes rapid energy transfer to form PMI^{T}, which itself has PMI^{-}–ep–Zn^{+} charge-transfer character or other spectral perturbations from the typical[41b] spectra of perylene triplets. The energetics are appropriate for PMI–ep–$Zn^{T} \rightarrow PMI^{T}$–ep–Zn triplet–triplet energy transfer (see Fig. 9A),[35a,41d,e,42] and a subnanosecond time scale for this process is consistent with the through-bond nature of energy transfer in these systems.

Fig. 5 shows time profiles for PMI–ep–Zn in toluene. The signal at 550 nm has an instrument-limited rise of PMI (0,0) bleaching, which results from photon absorption to directly prepare PMI*. The PMI bleaching then partially decays to the Zn–porphyrin Q(0,0)-bleaching amplitude resulting from PMI*–ep–Zn → PMI–ep–Zn* energy transfer. Although detailed analysis indicates that the decay time constant may be as short as ~0.2 ps, a PMI* lifetime of ≤0.4 ps is reported due to strong convolution of the PMI* decay with the instrument-response function. Similar data are found at 510 nm, where the instantaneous PMI (1,0) bleach gives way in ≤0.4 ps to the Zn* excited-state absorption in this region (Fig. 5B). The rapid formation of the Zn* transient absorption is most clearly seen at 460 nm, where there is no overlap with ground-state bleachings (Fig. 5C). Collectively, these data give a PMI* lifetime of ≤0.4 ps for PMI–ep–Zn in toluene (Table 2). In addition to the subpicosecond decay of PMI* and formation of Zn*, the data at several wavelengths (*e.g.* Fig. 5B) give a hint of a minor component with a time constant of ~3 ps. Such a component is also seen for the other dyads.

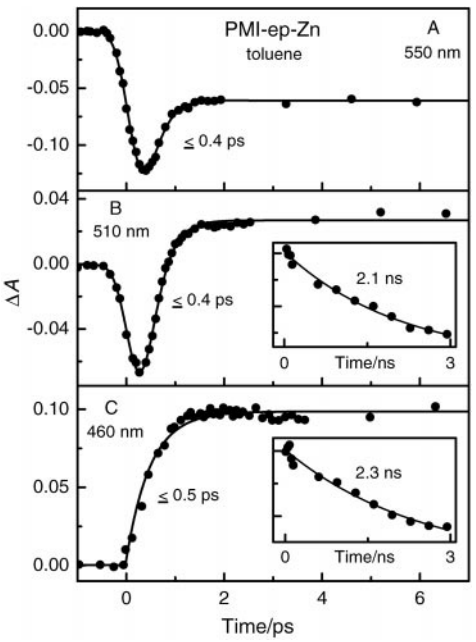

Fig. 5 Decay profiles of PMI–ep–Zn in toluene at room temperature upon excitation with a 130 fs 490 nm flash. The solid lines are fits to functions consisting of an instrument response and a fast exponential component (main panel) and a slow exponential decay (insets). Average values for the lifetimes of the appropriate excited states are discussed in the text and given in Table 2.

Among several sources considered, vibrational relaxation/equilibration in PMI and Zn* resulting from the ultrafast PMI*–ep–Por → PMI–ep–Por* energy-transfer process is likely the main contributor.[43]

As Zn* decays, the spectra in the vicinity of 510 and 460 nm evolve with time constants of ~2.1 ns and ~2.3 ns, respectively (Fig. 5, insets). Considering that the data span only about one 1/*e* time, these values are in excellent agreement with the time constant of 2.4 ns obtained from fluorescence decay. These results together afford a Zn* lifetime of 2.3 ± 0.2 ns for PMI–ep–Zn in toluene, which is basically the same as that of the isolated chromophore (Table 2).

PMI-ep. In order to obtain additional information on PMI excited-state spectra, data were acquired for the PMI-ep reference compound in toluene and iodobenzene, using excitation at 490 or 550 nm (Fig. 4B). The spectrum of PMI-ep in toluene at 5 ps (solid) can be assigned to PMI*, and has the same basic characteristics found in the spectrum at 0.3 ps for PMI–ep–Zn (Fig. 4A). Similar characteristics assignable to PMI* (albeit with reduced amplitude) are found at times extending to the ~3 ns limit of the measurements (Fig. 4B, dashed). The latter result is consistent with the fact that PMI* in PMI-ep decays almost quantitatively to the ground state *via* fluorescence emission ($\Phi_f = 0.95$; $\tau = 3.4$ ns; Table 2), with essentially no formation of the triplet state PMI^{T}.

In order to obtain information on the spectral characteristics of the perylene triplet excited state, data were acquired in iodobenzene, which should enhance $PMI^{*} \rightarrow PMI^{T}$ intersystem crossing *via* the heavy-atom effect. The PMI* spectrum for PMI-ep in iodobenzene at 5 ps (Fig. 4B inset, solid) is very similar to that found in toluene (Fig. 4B main panel, solid), except for small differences in wavelength due to the change in solvent. Notable features in the early-time spectrum in iodobenzene (as in toluene) are the PMI* Q(0,1) stimulated emission at ~615 nm, and the broad transient absorption centered at ~730 nm.

At 3 ns in iodobenzene, the PMI* stimulated emission is substantially reduced, and the broad transient absorption has shifted ~10 nm to shorter wavelengths. These characteristics (particularly the diminished stimulated emission) are consistent with PMI^{T} making a significant contribution to the 3 ns spectrum in iodobenzene. In keeping with this assessment, the PMI* lifetime and fluorescence yield are both reduced in iodobenzene ($\tau = (k_f + k_{isc} + k_{ic})^{-1} = 1.3$ ns; $\Phi_f = k_f \times \tau = 0.46$) relative to toluene ($\tau = 3.4$ ns; $\Phi_f = 0.95$), consistent with an enhanced rate constant of intersystem crossing (k_{isc}) expected for the heavy-atom solvent. The PMI^{T} characteristics for PMI-ep in iodobenzene (Fig. 4B inset, dashed) lack the large transient absorption band at ~615 nm found in the 2.5 ns spectrum for the PMI–ep–Zn dyad in toluene (Fig. 4A, dashed). Thus, to the extent that PMI^{T} (formed by energy transfer from Zn^{T}) contributes to the long-time spectrum in the dyad, the spectrum of the state must be perturbed by the presence of the linker and the porphyrin, perhaps with some PMI^{-}–ep–Zn^{+} charge-transfer character.

PMI–ep–Mg. The time-resolved absorption data for PMI–ep–Mg in toluene are generally similar to the results described above for PMI–ep–Zn (Fig. 6). The spectrum at 0.3 ps for PMI–ep–Mg can be assigned largely (but not completely) to PMI* based on the expected PMI bleaching and stimulated emission contributions. The spectrum also shows Mg* contributions at ~565 nm (Q(1,0) bleaching) and ~610 nm (Q(0,0) bleaching and stimulated emission). These porphyrin features overlap those due to perylene, but less extensively than for PMI–ep–Zn.

The PMI* lifetime for PMI–ep–Mg is extremely short, as was found for PMI–ep–Zn. A PMI* lifetime of ≤0.4 ps is determined at several wavelengths, as illustrated by the decay

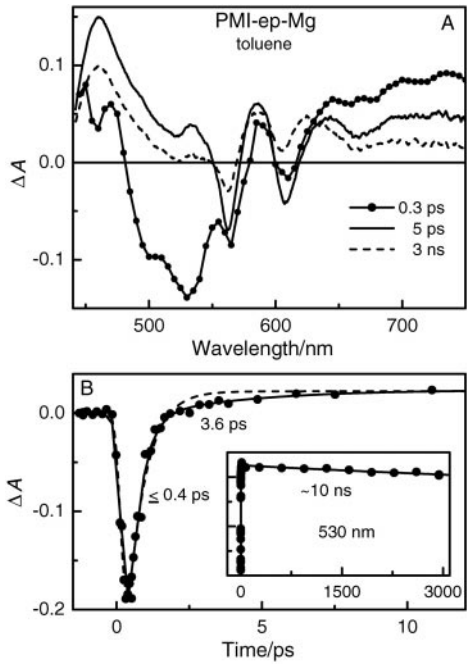

Fig. 6 Time-resolved absorption data for PMI–ep–Mg in toluene at room temperature, acquired using excitation with a 130 fs flash at 490 nm. (a) Spectra at various time delays. (b) Kinetic traces at 530 nm and a fit (solid line) consisting of the instrument response plus a three-exponential function with two fast components (main panel) and a slow decay (inset). The dashed line in the main panel shows that the fit is poorer if only one fast component is used. Average values for the lifetimes of the appropriate excited states are discussed in the text and given in Table 2.

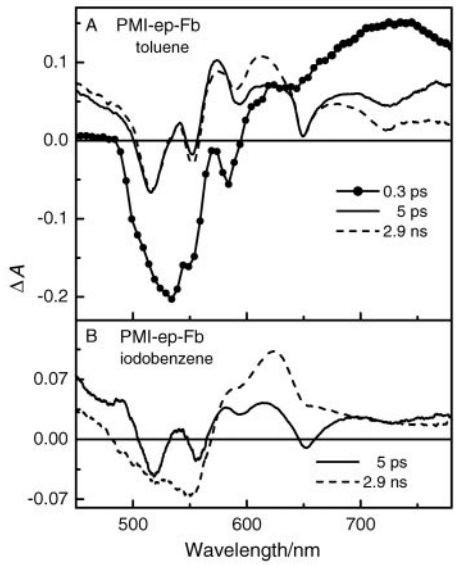

Fig. 7 Time-resolved absorption difference spectra for PMI–ep–Fb in (a) toluene and (b) iodobenzene. Conditions as in Fig. 4.

of the perylene bleaching at 530 nm in Fig. 6B. [Note also the presence of a minor second component to the early-time dynamics with a time constant of ~4 ps. Vibrational relaxation following decay of PMI* is the likely predominant origin of this component.[43]] Based on the ⩽0.4 ps PMI* lifetime and the static emission data described above, the PMI* decay primarily occurs by PMI*–ep–Mg → PMI–ep–Mg* energy transfer. The fast rate of this process is likely largely responsible for the small Mg–porphyrin contributions to the 0.3 ps spectrum.

The Mg* spectrum at 5 ps shows the expected bleaching and stimulated emission contributions at ~565 and ~610 nm (Fig. 6A, solid). The Mg* characteristics then decay with a time constant of ~10 ns (Fig. 6B inset), in good agreement with the Mg* lifetime of 9.6 ns for PMI–ep–Mg in toluene obtained by fluorescence decay (Table 2). As described above, this Mg* lifetime and the corresponding emission yield are only slightly perturbed from those for Mg–porphyrin reference compounds (Table 2). Thus, at 3 ns after excitation, Mg* has only partially decayed, almost certainly largely (80–90%) by intersystem crossing to Mg^T as in the isolated chromophore.[40] This modest level of decay is consistent with the similar characteristics in the 3 ns and 5 ps spectra (Fig. 6A, dashed and solid spectra).

PMI–ep–Fb in toluene. Fig. 7A shows transient absorption spectra for PMI–ep–Fb in toluene. Data were acquired using 130 fs flashes at 490 nm that primarily excite the perylene, or with 550 nm flashes; the spectra with the two excitation wavelengths agree well in the regions of overlap (570–670 nm). The spectrum at 0.3 ps can be assigned primarily to PMI*, as it is dominated by bleaching of the PMI (1,0) and (0,0) ground-state absorption bands (490, 530 nm) and PMI (0,0) and (0,1) stimulated emission (530 and 580 nm). In analogy to the metalloporphyrin-containing dyads, Fb* also appears to contribute to the 0.3 ps spectrum. Again, the porphyrin contributions at this early time likely arise primarily because the PMI* decay (by energy transfer to Fb) is so fast that it has already occurred to some extent at this time.

The Fb* characteristics dominate the spectrum at 5 ps after excitation (Fig. 7A, solid). These features include bleaching of the porphyrin $Q_y(1,0)$, $Q_y(0,0)$, and $Q_x(1,0)$ ground-state absorption bands at 515, 550, and 585 nm, respectively. The feature at 645 nm contains both $Q_x(0,0)$ bleaching and stimulated emission, and the trough at 715 nm is $Q_x(0,1)$ stimulated emission. These features are all expected based on the bands in the Fb-porphyrin static optical spectra (see *e.g.*, Fig. 2E and refs. 16, 20).

The spectrum at 5 ps evolves into that shown at 2.9 ns in Fig. 7 (dashed). Many of the Fb-porphyrin bleachings remain (because Fb* decay occurs on a timescale of ~10 ns), but the amplitudes of the stimulated emission contributions at 645 and 715 nm (relative to the transient absorption) appear to decrease slightly. Furthermore, an absorption band at ~615 nm develops, which is analogous to the feature formed as Zn* decays in PMI–ep–Zn in toluene (Fig. 4A). It is similarly likely that the 2.9 ns spectrum in Fig. 7 reflects Fb^T (formed by intersystem crossing from Fb* as in the isolated Fb porphyrin with 70–80% yield[40]) or PMI^T (formed by rapid energy transfer from Fb^T). The spectrum of either triplet excited state would be perturbed from that of the isolated pigment[41] due to the perylene–porphyrin interactions in the dyad, perhaps including PMI^-–ep–Fb^+ charge-transfer character.

Fig. 8 shows time profiles for PMI–ep–Fb in toluene excited with a 130 fs flash at 490 nm (which primarily pumps the perylene component). Fig. 8A shows the instrument-limited formation of (0,0) PMI bleaching and PMI* stimulated emission at 530 nm, followed by decay of these characteristics with a time constant of ~0.5 ps. Fig. 8D gives the analogous instrument-limited formation of PMI* transient absorption at 650 nm and decay with a time constant of ~0.6 ps. At intermediate wavelengths, PMI* characteristics form instantaneously and decay to those for Fb* in ⩽0.4 ps (Fig. 8B and C). Collectively, these data give a PMI* lifetime of 0.4 ± 0.2 ps for PMI–ep–Fb in toluene. The kinetic traces at 575 and 615 nm also indicate the presence of a minor, ~2.5 ps component, which likely represents mainly vibrational equilibration, as discussed above for the other dyads.[43] The subsequent decay of Fb* and formation of its decay products occurs with a time constant of ~13 ns (Fig. 8C, inset). This value is in good

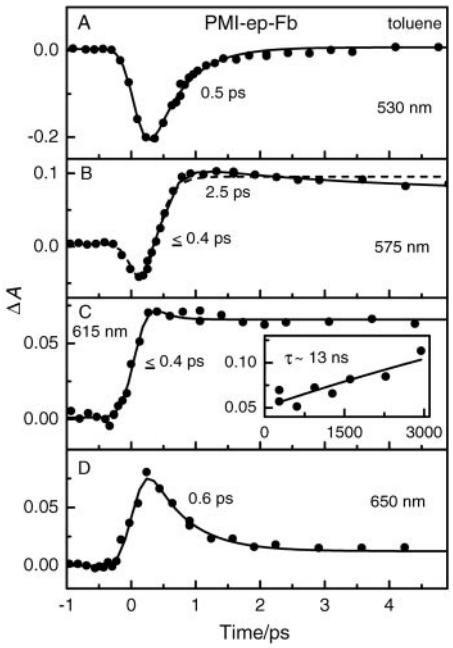

Fig. 8 Decay profiles of PMI–ep–Fb in toluene at room temperature upon excitation with a 130 fs 490 nm flash. The lines are fits to functions consisting of an instrument response plus (a) a single component, (b) a single component (dashed) or two components (solid), (c) two fast components (main panel) and a slow decay (inset), and (d) a single decay component. Average values for the lifetimes of the appropriate excited states are discussed in the text and given in Table 2.

agreement with the Fb* lifetime of 12.3 ns for PMI–ep–Fb in toluene determined by fluorescence decay (Table 2).

PMI–ep–Fb in iodobenzene. Measurements were also performed on PMI–ep–Fb in iodobenzene, which should enhance $Fb^* \rightarrow Fb^T$ intersystem crossing *via* the heavy-atom effect. The absorption difference spectrum at 5 ps in this solvent (Fig. 7B, solid) is very similar to that at the same time in toluene (Fig. 7A, solid) and can be similarly ascribed to Fb*. Fluorescence measurements indicate that Fb* decays with a time constant of 1.4 ns in iodobenzene compared to 12.3 ns in toluene, consistent with enhanced intersystem crossing to Fb^T. Thus, Fb* should have decayed significantly by 2.9 ns, and with a Fb^T yield at least as great as $\Phi_T = 0.7$–0.8 for the isolated porphyrin[40] (Fig. 7b, dashed). However, the spectrum at 2.9 ns is more complex than might be expected for Fb^T based on studies of isolated porphyrins.[41a]

The 2.9 ns spectrum in iodobenzene shows (1) diminished amplitude of the combined bleaching/stimulated-emission feature at ~650 nm present in the 5 ps Fb* spectrum, (2) a prominent transient absorption band at ~615 nm similar to that seen in the long-time spectrum in toluene (Fig. 7A *versus* 7B, dashed), and (3) bleaching of the perylene (0,0) band at 530 nm that fills in the region between the Fb bleachings at 515 and 550 nm (compare spectrum at 2.9 ns with the Fb* spectrum at 5 ps). Collectively, these data are consistent with enhanced $PMI–ep–Fb^* \rightarrow PMI–ep–Fb^T$ intersystem crossing in iodobenzene compared to toluene, followed by more significant $PMI–ep–Fb^T \rightarrow PMI^T–ep–Fb$ energy transfer by ~3 ns in the heavy-atom solvent.

Discussion

One of the primary objectives in designing the PMI–ep–Por (Por = Zn, Mg, Fb) dyads was to improve upon the light-harvesting capabilities exhibited by the PDI–pep–Por dyads.[14,15] This goal has been successfully attained in the PMI–ep–Por dyads in toluene. In many respects, these systems represent ideal units for light input and subsequent light emission or energy transmission to other elements in larger architectures. In particular, the PMI–ep–Por dyads exhibit the following general features. (1) The PMI–ep–Por dyads retain the favorable antenna properties of the PDI–pep–Por arrays, whereby the strong blue–green absorption of the perylene accessory chromophore complements the absorption properties of the porphyrin (Fig. 2 and 3). (2) The PMI-based arrays have substantially increased rates ($k_{ENT} \geqslant (0.5\ ps)^{-1}$) and efficiencies ($\Phi_{ENT} > 95\%$) of energy transfer from perylene to porphyrin, even compared to the most favorable PDI-based light-harvesting array (PDI–pep–Fb; $k_{ENT} \sim (3\ ps)^{-1}$, $\Phi_{ENT} \sim 85\%$). (3) The excited porphyrin in the PMI-based arrays (obtained by energy transfer from perylene or by direct photon absorption) has a fluorescence lifetime and yield basically the same as in the isolated chromophore (as is also the case in PDI–pep–Fb[15]). In other words, in nonpolar media Por* is not quenched by deleterious reactions involving the PMI accessory pigment that would compromise light-harvesting and energy-utilization processes.

In the following sections, we elaborate on the general features of the PMI–ep–Por dyads noted above. These points are described in terms of (1) the electronic manifolds and excited-state processes of the dyads in toluene, (2) the origins of the enhanced electronic communication in the PMI–ep–Por dyads relative to the PDI–pep–Por analogs, and (3) the implications for use of these dyads in molecular photonics.

Energies and photoprocesses of the electronic states

Fig. 9 shows the electronic manifolds and key light-induced processes for each of the PMI–ep–Por (Por = Zn, Mg, Fb) dyads in toluene. The PMI* and Por* excited-state energies (eV, in parentheses) were obtained by averaging the energies of the corresponding (0,0) absorption and fluorescence features in the arrays or relevant reference compounds (Fig. 2 and 3). For each dyad, the $PMI^-–ep–Por^+$ charge-separated state is placed 0.37 eV higher than the analogous $PDI^-–pep–Por^+$ state. This shift reflects the fact that the perylene monoimide in PMI–ep–Zn is more difficult to reduce than the perylene diimide in PDI–pep–Zn by 0.37 eV (similarly, the reduction potential is 0.43 V more negative in the PMI-m *versus* PDI-m reference compounds) (Table 1). The $PDI^-–pep–Por^+$ energies were obtained in our previous studies of the PDI-based arrays from porphyrin redox potentials and a direct measurement of the $PDI^-–pep–Zn^+$ energy from delayed-fluorescence data.[14,15] Accordingly, $PMI^-–ep–Fb^+$ in toluene lies 0.33 eV above PMI* (and 0.67 eV above Fb*), $PMI^-–ep–Zn^+$ lies 0.18 eV above PMI* (and 0.33 eV above Zn*), and $PMI^-–ep–Mg^+$ lies 0.03 eV above PMI* (and 0.24 eV above Mg*).

The energetics of the excited states and charge-separated states indicate that photoinduced $PMI^*–ep–Por \rightarrow PMI^-–ep–Por^+$ hole transfer cannot occur in the PMI-based arrays in toluene. Similarly, $PMI–ep–Por^* \rightarrow PMI^-–ep–Por^+$ electron transfer is prohibited in all three arrays. Thus, except for the processes that can occur in the isolated pigments, $PMI^*–ep–Por \rightarrow PMI–ep–Por^*$ energy transfer is the only excited-singlet-state process operable to any appreciable degree in the PMI–ep–Por dyads in nonpolar media. These expectations are fully consistent with the experimental results, and represent a major change from the corresponding PDI–pep–Por dyads in toluene. For the latter dyads, charge-transfer processes are operable even in nonpolar solvents (and the extent varies with the porphyrin).[14,15] This major difference between the two classes of dyads results primarily from the higher energies of the $PMI^-–ep–Por^+$ *versus* $PDI^-–pep–Por^+$ charge-separated states (see Fig. 1).

The microscopic rate constants and yields of $PMI^*–ep–Por \rightarrow PMI–ep–Por^*$ energy transfer in the arrays can be obtained from the static fluorescence or time-resolved optical

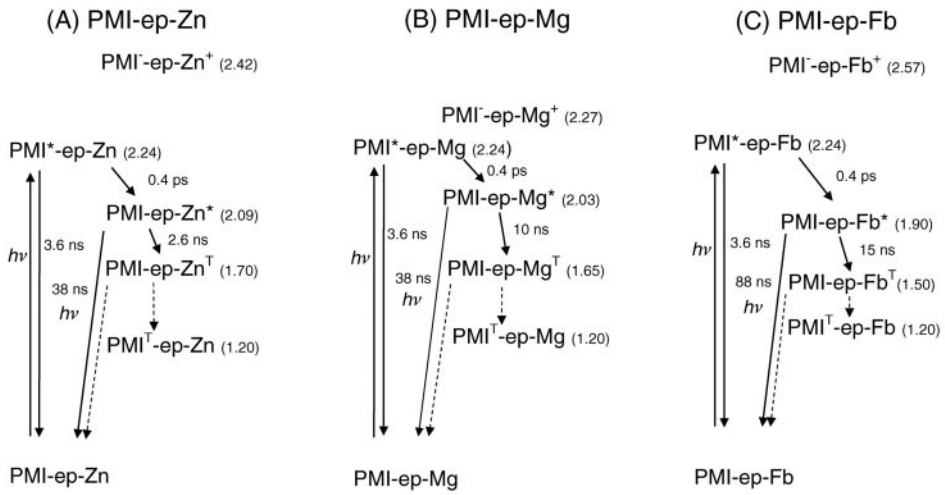

Fig. 9 Schematic energy diagram and processes for the PMI–ep–Por dyads in toluene at room temperature. The energies of the various states (in eV) and the rate constants for the processes were derived as discussed in the text.

data using the equations and methods described previously (with consideration of the effects of porphyrin–perylene interactions on the microscopic rate constants).[14] However, even without a rigorous analysis, the rate constant for energy transfer from perylene to porphyrin in each of the PMI–ep–Por arrays in toluene is easily seen to be $k_{ENT} \geqslant (0.5\ ps)^{-1}$, and the efficiency is conservatively placed at $\Phi_{ENT} > 95\%$ (and is likely $>99\%$). These estimates derive from the following observations: (1) the PMI* lifetime of $\leqslant 0.4$ ps in the arrays is considerably shorter than the value of 3.4 ns in the PMI-ep reference compound, and the PMI* fluorescence yield is similarly reduced (Table 2). These results imply that at least one PMI* process not present in the monomer is very efficient in the dyad. (2) The porphyrin fluorescence intensity obtained using perylene excitation is the same within experimental error as the yield measured with direct porphyrin excitation (Table 2), suggesting that energy transfer from perylene to porphyrin is essentially quantitative. Points 1 and 2 together show that the energy-transfer process dominates the reduction in PMI* lifetime and fluorescence in the dyads. (3) In agreement with this assessment, the transient absorption data show no clear evidence for significant contributions of alternative PMI* decay pathways such as hole transfer to the porphyrin. Collectively, these findings indicate that PMI*–ep–Por $\rightarrow$ PMI–ep–Por* energy transfer is an ultrafast ($k_{ENT} \geqslant (0.5\ ps)^{-1}$) and effectively quantitative process in the PMI–ep–Por dyads in nonpolar media.

The data for each of the three PMI–ep–Por dyads also show that once perylene-to-porphyrin energy transfer has occurred, the Por* state decays in a manner similar to that in the isolated porphyrin (with similar microscopic rates for the decay pathways). The only perturbations to the Por* spectral and dynamic properties in each dyad relative to the reference compounds are consistently explained by a small change in the radiative rate constant (k_f) resulting from strong electronic interactions involving the components of the array. In analogy with the isolated porphyrins, the primary (70–90%) decay pathway of Por* in the PMI–ep–Por dyads in toluene is intersystem crossing to the Por^T triplet excited state.[40] A new process for which there is significant evidence in these dyads is subsequent, subnanosecond triplet–triplet energy transfer from Por^T to the ground-state perylene to form PMI^T. The energetics for this process are appropriate, based on the triplet energies for the isolated pigments and related reference compounds (Fig. 9).[35a,41d,e,42] We have not observed such a triplet–triplet energy-transfer process in any of our previous studies of photoinduced energy transfer involving two porphyrins or a porphyrin plus accessory pigment. In those cases, the singlet–triplet splittings in the components are such that the chromophore that serves as the singlet–singlet energy-transfer acceptor also has the lower energy triplet excited state. Thus, triplet–triplet energy transfer in the reverse direction cannot occur, as it can in the PMI–ep–Por dyads studied here.

Perylene–porphyrin electronic communication in the PMI–ep–Por dyads

Excited-state energy transfer is much faster in the PMI–ep–Por dyads than in the PDI–pep–Por analogs ($k_{ENT} \geqslant (0.5\ ps)^{-1}$ *versus* $\sim(3\ ps)^{-1}$). In addition to the change in linker (ep *versus* pep), this difference in energy-transfer rates derives from attachment to perylene at a site with much higher electron density (core C9 *versus* *N*-imide; Chart 1). The frontier molecular orbitals have larger coefficients at the perylene C9 *versus* *N*-imide positions. This fact is supported by both calculations and experimental results, including substituent effects on the optical spectra. Such effects have been obtained previously[23,24] and in our studies of the PMI–ep–Por and PDI–pep–Por dyads and reference compounds (Fig. 2 and 3 and refs. 14, 15). For example, the absorption and emission spectra of the PDI-m reference compound are basically unchanged upon attachment of the linker (or linker plus porphyrin) to the PDI *N*-imide position. In contrast, the corresponding optical bands of PMI-m are substantially red-shifted upon attachment of the ethyne to the PMI C9 position, and further shifted with successive addition of the linker phenyl ring and then the porphyrin.

The above observations are indicative of the strong electronic communication that extends from the perylene *via* its C9 position, through each element of the linker, to the porphyrin. [Recall that this communication is primarily in the excited state because the ground-state redox potentials of PMI are not significantly affected by addition of the linker and phenyl rings.] Furthermore, the spectral and kinetic data taken as a whole indicate that the effective perylene–porphyrin electronic coupling is stronger for PMI–ep–Zn and PMI–ep–Mg compared to PMI–ep–Fb. This latter observation may reflect differences in the electron density of the relevant frontier molecular orbitals at the *meso*-carbon to which the linker is attached, and may be influenced by the difference in symmetry of the metalloporphyrin *versus* the free base porphyrin (metalloporphyrin, $\sim D_{4h}$; free base porphyrin, $\sim D_{2h}$).

The effects of the perylene attachment site on the spectra and excited-state-dynamics in the PMI–ep–Por *versus* PDI–pep–Por arrays complement our previous work on the effects of the porphyrin–linker attachment motif on the rates of inter-porphyrin energy transfer.[17,19,21] The rates of linker-mediated

(through-bond[16,17]) energy transfer in the porphyrin–porphyrin systems correlate with the use of positions of high *versus* low electron density in the frontier molecular orbitals of the porphyrin and linker. Here, we have applied this same logic to the perylene–linker attachment motif, together with a shorter linker, to push the rates of perylene-to-porphyrin energy transfer into the subpicosecond regime.

Implications for photonic devices

The results presented here for the PMI–ep–Por dyads represent the fruits of a successful design approach based on a thorough understanding of the factors underlying the mechanisms, rates, and yields of photoinduced energy transfer in porphyrin-based arrays. We have extended knowledge of the effects of porphyrin–linker attachment motif and molecular-orbital electron-density distributions to the perylene accessory pigment. In so doing, we have greatly increased the rates and efficiencies of energy transfer in the PMI–ep–Por arrays relative to the PDI–pep–Por analogs studied in the first two papers in this series.[14,15] Our previous studies of the PDI–pep–Por arrays revealed a multitude of interrelated energy-transfer and charge-transfer phenomena, the relative importance of which could be tuned to a certain extent using variations in the redox properties of the porphyrin component. Here, we have extended these insights to tuning the perylene accessory pigment in order to essentially preclude all photoinduced charge-transfer phenomena for the PMI–ep–Por arrays in nonpolar media.

Consequently, the perylene accessory chromophore (and its linker–attachment motif) in the PMI-based arrays (1) complements the absorption properties of the porphyrin, (2) allows ultrafast and effectively quantitative energy transfer to the porphyrin, and (3) avoids quenching of the excited porphyrin (which would diminish the ability of the constructs to harvest light and then emit light or transfer energy to other stages in molecular devices). Thus, the PMI–ep–Por dyads are excellent units for light-harvesting and energy-utilization functions. As will be shown in a forthcoming paper,[39] ultrafast and highly efficient charge-transfer and charge-recombination processes can be achieved when these same dyads are in placed in polar media, affording utility for molecular switching or clocking functions. Collectively, our studies of the PDI–pep–Por and PMI–ep–Por arrays have provided insights and concrete examples of tunable arrays that can be incorporated into more elaborate architectures for use in a variety of molecular optoelectronics applications.

Experimental

General

^{1}H NMR spectra were collected at 300 MHz. Products were analyzed by fast-atom bombardment (FAB) or by laser desorption mass spectrometry in the absence of a matrix (LD-MS).[44] Absorption and emission spectra were routinely obtained in toluene. Unless otherwise indicated, all reagents were obtained from Aldrich Chemical Company, Milwaukee, WI, and all solvents were obtained from Fisher Scientific.

PMI–ep–Mg

A mixture of PMI–ep–Fb (8.3 mg, 6.2 μmol) and MgI_2 (200 mg, 0.72 mmol) in CH_2Cl_2 at room temperature was stirred for 5 min. Then *N,N*-diisopropylethylamine (125 μL, 0.72 mmol) was added and the reaction mixture was stirred for 2 h (with monitoring by fluorescence spectroscopy). The crude reaction mixture was dissolved in CH_2Cl_2 (50 mL), washed with water, dried (Na_2SO_4), evaporated to dryness, chromatographed (alumina, CH_2Cl_2–hexanes, 2 : 1), and recrystallized (ethanol) to afford a purple solid (7.2 mg, 88%). ^{1}H NMR (THF-d_8) δ 1.17–1.40 (m, 18H), 1.75–1.94 (m, 18H), 2.51–2.62 (m, 9H), 7.13 (d, 1H, J = 2.4 Hz), 7.27–7.33 (m, 6H), 7.38–7.45 (m, 1H), 7.54–7.59 (m, 1H), 7.85–7.93 (m, 1H), 8.04–8.17 (m, 3H), 8.28–8.35 (m, 2H), 8.51–8.85 (m, 15H); LD-MS obsd 1297.8, 1229.2 [$M^+ - 2(C(CH_3)_3)$]; FAB-MS obsd 1293.57, calcd exact mass, 1293.58 ($C_{91}H_{75}N_5O_2Mg$); λ_{abs} 427, 530, 564, 607 nm; λ_{em} 619, 666 nm.

Characterization

The electrochemical and spectroscopic methods employed are described in the first paper in this series.[14]

Acknowledgements

This research was supported by the NSF (CHE-9707995 and CHE-9988142) (D.F.B., D.H., and J.S.L). Partial funding for the Mass Spectrometry Laboratory for Biotechnology at North Carolina State University was obtained from the North Carolina Biotechnology Center and the NSF. P.S. thanks Cochin University of Science and Technology for a sabbatical leave.

References

1 M. P. O'Neil, M. P. Niemczyk, W. A. Svec, D. Gosztola, G. L. Gaines III and M. R. Wasielewski, *Science*, 1992, **257**, 63.
2 E. M. Just and M. R. Wasielewski, *Superlattices Microstr.*, 2000, **28**, 317.
3 D. Gosztola, M. P. Niemczyk and M. R. Wasielewski, *J. Am. Chem. Soc.*, 1998, **120**, 5118.
4 H. Zollinger, *Color Chemistry: Syntheses, Properties, and Applications of Organic Dyes and Pigments*, VCH, Weinheim, 1991.
5 H. R. Kerp, H. Donker, R. B. M. Koehorst, T. J. Schaafsma and E. E. van Faassen, *Chem. Phys. Lett.*, 1998, **298**, 302.
6 H. Tian, P.-H. Liu, W. Zhu, E. Gao, D.-J. Wu and S. Cai, *J. Mater. Chem.*, 2000, **10**, 2708.
7 H. Langhals and J. Gold, *J. Prakt. Chem.*, 1996, **338**, 654.
8 H. Langhals and J. Gold, *Liebigs Ann.*, 1997, 1151.
9 H. Langhals and W. Jona, *Angew. Chem., Int. Ed.*, 1998, **37**, 952.
10 F. Würthner and A. Sautter, *Chem. Commun.*, 2000, 445.
11 S.-G. Liu, Y.-Q. Liu, Y. Xu, X.-Z. Jiang and D.-B. Zhu, *Tetrahedron Lett.*, 1998, **39**, 4271.
12 M. R. Wasielewski, D. Gosztola and W. A. Svec, *Mol. Cryst. Liq. Cryst.*, 1994, **253**, 289.
13 M. A. Miller, R. K. Lammi, S. Prathapan, D. Holten and J. S. Lindsey, *J. Org. Chem.*, 2000, **65**, 6634.
14 S. Prathapan, S. I. Yang, J. Seth, M. A. Miller, D. F. Bocian, D. Holten and J. S. Lindsey, *J. Phys. Chem. B*, in the press (Paper 1 in this series).
15 S. I. Yang, S. Prathapan, M. A. Miller, J. Seth, D. F. Bocian, J. S. Lindsey and D. Holten, *J. Phys. Chem. B*, in the press (Paper 2 in this series).
16 J.-S. Hsiao, B. P. Krueger, R. W. Wagner, T. E. Johnson, J. K. Delaney, D. C. Mauzerall, G. R. Fleming, J. S. Lindsey, D. F. Bocian and R. J. Donohoe, *J. Am. Chem. Soc.*, 1996, **118**, 11181.
17 J. P. Strachan, S. Gentemann, J. Seth, W. A. Kalsbeck, J. S. Lindsey, D. Holten and D. F. Bocian, *J. Am. Chem. Soc.*, 1997, **119**, 11191.
18 F. Li, S. Gentemann, W. A. Kalsbeck, J. Seth, J. S. Lindsey, D. Holten and D. F. Bocian, *J. Mater. Chem.*, 1997, **7**, 1245.
19 S. I. Yang, J. Seth, T. Balasubramanian, D. Kim, J. S. Lindsey, D. Holten and D. F. Bocian, *J. Am. Chem. Soc.*, 1999, **121**, 4008.
20 P. Hascoat, S. I. Yang, R. K. Lammi, J. Alley, D. F. Bocian, J. S. Lindsey and D. Holten, *Inorg. Chem.*, 1999, **38**, 4849.
21 R. K. Lammi, A. Ambroise, T. Balasubramanian, R. W. Wagner, D. F. Bocian, D. Holten and J. S. Lindsey, *J. Am. Chem. Soc.*, 2000, **122**, 7579.
22 (*a*) J. Seth, V. Palaniappan, T. E. Johnson, S. Prathapan, J. S. Lindsey and D. F. Bocian, *J. Am. Chem. Soc.*, 1994, **116**, 10578; (*b*) J. Seth, V. Palaniappan, R. W. Wagner, T. E. Johnson, J. S. Lindsey and D. F. Bocian, *J. Am. Chem. Soc.*, 1996, **118**, 11194.
23 M. Adachi, Y. Murata and S. Nakamura, *J. Phys. Chem.*, 1995, **99**, 14240.

24 H. Langhals, S. Demmig and H. Huber, *Spectrochim. Acta*, 1988, **44A**, 1189.
25 J. S. Lindsey and J. N. Woodford, *Inorg. Chem.*, 1995, **34**, 1063.
26 L. Feiler, H. Langhals and K. Polborn, *Liebigs Ann.*, 1995, 1229.
27 R. W. Wagner, T. E. Johnson, F. Li and J. S. Lindsey, *J. Org. Chem.*, 1995, **60**, 5266.
28 R. W. Wagner, T. E. Johnson and J. S. Lindsey, *J. Am. Chem. Soc.*, 1996, **118**, 11166.
29 D. Gosztola, M. P. Niemczyk, W. Svec, A. S. Lukas and M. R. Wasielewski, *J. Phys. Chem. A*, 2000, **104**, 6545.
30 R. H. Felton, in *The Porphyrins*, ed. D. Dolphin, Academic Press, New York, 1978, Vol. V, pp. 53–126.
31 (*a*) J. Salbeck, H. Kunkely, H. Langhals, R. W. Saalfrank and J. Daub, *Chimia*, 1989, **43**, 6; (*b*) W. E. Ford, H. Hiratsuka and P. V. Kamat, *J. Phys. Chem.*, 1989, **93**, 6692.
32 The PMI absorption contour in the dyads and reference compounds has less overall structure than for PDI-based analogs (Fig. 2 and 3 and refs. 14 and 15). This effect could arise for several reasons, including larger differences in equilibrium structure between the ground and excited states, more excited-state charge-transfer character, or more Franck–Condon intensity shifted into lower frequency modes for the PMI- *versus* PDI-containing arrays..
33 (*a*) Differences in the porphyrin Q(0,0)/Q(1,0) absorption-intensity ratio in the dyads *versus* reference compounds are difficult to assess due to porphyrin–perylene spectral overlap. The effect would reflect differences in the radiative rate constant (k_f)[33b] in the dyads, which are clearly indicated by the intensity ratios in the fluorescence spectra; (*b*) I. Yang, J. Seth, J.-P. Strachan, S. Gentemann, D. H. Kim, D. Holten, J. S. Lindsey and D. F. Bocian *J. Porphyrins Phthalocyanines*, 1999, **3**, 117.
34 The minor perylene emission that is observed in the dyads appears to come from trace (<0.1%) unsubstituted perylene monomer and not from the perylene in the dyad, judging from the positions of the emission bands relative to the reference compounds (see Fig. 2).
35 (*a*) The Zn* fluorescence yields and lifetimes in Table 2 afford porphyrin natural radiative rate constants of $k_f = \Phi_f/\tau = 0.070/2.3\ \text{ns} = (33\ \text{ns})^{-1}$ for the dyad and $0.035/2.4\ \text{ns} = (69\ \text{ns})^{-1}$ for ZnU′. [The latter value is in good agreement with the typical $k_f \sim (60\ \text{ns})^{-1}$ for metalloporphyrin monomers.[35b]] Assuming that the intersystem crossing and internal conversion rate constants (k_{isc} and k_{ic}) for Zn* decay are the same in PMI–ep–Zn and ZnU′, the fluorescence lifetimes ($\tau = (k_f + k_{isc} + k_{ic})^{-1}$) and yields ($\Phi_f = k_f \times \tau$) indicate that the radiative rate constant k_f is 2-fold greater in the dyad (assuming that k_{ic} and k_{isc} are the same as in the isolated porphyrin). Similarly, the ratio of the porphyrin Q(0,0) and Q(0,1) emission features is altered in the dyad *versus* the monomer (Fig. 2A *versus* Fig. 2E). If the Q(0,1) emission band is used as a normalizer,[33b] then the increased Q(0,0) intensity corresponds to a 1.8-fold increase in k_f for porphyrin fluorescence in PMI–ep–Zn versus ZnU′. Thus, the fluorescence spectrum and yield/lifetime results are in good quantitative agreement in showing that the inherent porphyrin radiative characteristics are perturbed in the dyad relative to the isolated chromophore; (*b*) M. Gouterman, in *The Porphyrins*; ed. D. Dolphin, Academic Press, New York, 1978, Vol. III, pp. 1–165.
36 The Mg* fluorescence yields in PMI–ep–Mg *versus* MgU′ ($\Phi_f = 0.24$ *versus* 0.16) and the corresponding fluorescence lifetimes ($\tau = 9.1 \pm 0.9$ *versus* 10.0 ± 0.8 ns) give a 1.6-fold larger radiative rate constant in the dyad ($k_f = (38\ \text{ns})^{-1}$ *versus* $(62\ \text{ns})^{-1}$). A similar, 1.4-fold increase in k_f is indicated by the larger Q(0,0)/Q(0,1) ratio for the porphyrin fluorescence in PMI–ep–Mg *versus* MgU′ or PDI–pep–Mg (Fig. 3C, 3D and refs. 18 and 20).
37 The Fb* radiative rate is calculated to be only ~1.2-fold larger in PMI–ep–Fb *versus* FbU′ from the emission yields and lifetimes (Table 2), and about the same in these two compounds and in PDI–ep–Fb based on the nearly identical Q(0,0)/Q(0,1) fluorescence-intensity ratios and Q(0,0)/Q(1,0) absorption-intensity ratios (Fig. 3E, 3F, and refs. 16 and 20).
38 The PMI* decay is so fast ($\leqslant$0.4 ps) that the raw spectra are distorted due to the dispersion in arrival times at the sample of the different wavelengths in the probe pulse. In other words, by the time the probe light has arrived on the red edge of the spectral window shown, the absorption characteristics of PMI* initially present on the blue edge of the spectrum have already decayed to some extent. Thus, the PMI* spectrum is constructed using the initial amplitude (immediately after the instrument response) of ΔA at each wavelength obtained from analysis of the associated kinetic trace.
39 S. I. Yang, R. K. Lammi, S. Prathapan, M. A. Miller, J. Seth, J. R. Diers, D. F. Bocian, J. S. Lindsey and D. Holten, manuscript in preparation.
40 (*a*) A. T. Gradyushko, A. N. Sevchenko, K. N. Solovyov and M. P. Tsvirko, *Photochem. Photobiol.*, 1970, **11**, 387; (*b*) Y. Kajii, K. Obi, I. Tanaka and S. Tobita, *Chem. Phys. Lett.*, 1984, **111**, 347; (*c*) K. Kikuchi, Y. Kurabayashi, H. Kokubun, Y. Kaizu and H. Kobayashi, *J. Photochem. Photobiol. A: Chem.*, 1988, **45**, 261; (*d*) R. D. Bonnett, D. McGarvey, A. Harriman, E. J. Land, T. G. Truscott and U. J. Winfield, *Photochem. Photobiol.*, 1988, **48**, 271; (*e*) B. M. Dzhagarov, *Opt. Spektrosk.*, 1970, **28**, 66; (*f*) K. Hurley, N. Sinai and H. Linschitz, *Photochem. Photobiol.*, 1983, **38**, 9.
41 (*a*) Absorption difference spectra of porphyrin excited triplet states normally have relatively featureless absorption between ~500 and 700 nm, with one or more small features to longer wavelengths[41c]; (*b*) Absorption difference spectra of perylene excited triplet states appear to have one or more reasonably strong absorption bands to the blue of ~600 nm, with weaker absorption to longer wavelengths[41d,e]; (*c*) J. Rodriguez, C. Kirmaier and D. Holten, *J. Am. Chem. Soc.*, 1989, **111**, 6500; (*d*) W. E. Ford and P. V. Kamat, *J. Phys. Chem.*, 1987, **91**, 6373; (*e*) M. Sadrai, L. Hadel, R. R. Sauers, S. Husain, K. Krogh-Jesperson, J. D. Westbrook and G. R. Bird, *J. Phys. Chem.*, 1992, **96**, 7988.
42 A. T. Gradyushko and M. P. Tsvirko, *Optics Spectrosc.*, 1971, **31**, 291.
43 Internal vibrational energy redistribution and cooling *via* flow of energy to the solvent are expected within PMI or Por* following the ultrafast, downhill energy transfer from PMI* to the porphyrin. This equilibration process is known to extend onto the picosecond time scale and even to tens of picoseconds (depending on the system and excess energy) and to cause corresponding effects on the optical spectra and complex, detection-wavelength-dependent kinetic data: J. Rodriguez, C. Kirmaier and D. Holten, *Chem. Phys.*, 1991, **94**, 6020.
44 (*a*) N. Srinivasan, C. A. Haney, J. S. Lindsey, W. Zhang and B. T. Chait, *J. Porphyrins Phthalocyanines*, 1999, **3**, 283; (*b*) D. Fenyo, B. T. Chait, T. E. Johnson and J. S. Lindsey, *J. Porphyrins Phthalocyanines*, 1997, **1**, 93.